# Observation of Unusual Hysteretic Magnetic Properties of the Rare Earth Intermetallic Compound $PrMnSi_2$: Magnetic Susceptibility, Magnetization, Heat Capacity, and Electronic Band Structure Studies

Sang-Hwan Kim and Dong-Kyun Seo*

*Department of Chemistry and Biochemistry, Arizona State University, Tempe, Arizona 85287-1604*

Reinhard K. Kremer and Jürgen Köhler*

*Max-Planck-Institut für Festkörperforschung, Heisenbergstrasse 1, D-70569 Stuttgart, Germany*

Antoine Villesuzanne*,† and Myung-Hwan Whangbo*

*Department of Chemistry, North Carolina State University, Raleigh, North Carolina 27695-8204*

*Received March 22, 2005. Revised Manuscript Received May 4, 2005*

The magnetic properties of the rare earth intermetallic compound $PrMnSi_2$ were characterized by carrying out magnetic susceptibility, magnetization, and heat capacity measurements and performing APW+lo/LDA+$U$ electronic band structure calculations for several ordered spin states of $PrMnSi_2$. The temperature dependence of the magnetic susceptibilities shows strong hysteresis at low magnetic fields and exhibits hysteresis under magnetic fields up to ~5 T. The magnetizations present unusual hysteresis loops as a function of temperature. The magnetic susceptibility and heat capacity measurements reveal that $PrMnSi_2$ undergoes three magnetic phase transitions, one below ~50 K and two below ~20 K. The probable causes for the observed anomalous magnetic properties were discussed on the basis of nearly degenerate ordered spin states found from electronic structure calculations.

## 1. Introduction

The rare earth intermetallic compound $PrMnSi_2$ consists of two-dimensional square-net layers made up of Mn atoms.[1] These Mn layers sandwich parallel silicon-ribbon chains such that the terminal Si atoms cap the $Mn_4$ squares of each Mn layer to form $Mn_4Si$ tetragonal pyramids (Figure 1). The Pr atoms reside in the "$Si_{10}Mn_4$" cages located between two adjacent Si-ribbon chains and the Mn layers so that each Mn is tetrahedrally surrounded by four Si atoms and four Pr atoms. There occur two separate layers of Pr atoms between two adjacent Mn layers so that the layers of the magnetic atoms Mn and Pr repeat in the sequence $(-Pr-Mn-Pr-)_\infty$ along the $b$-direction. The compound $PrMnSi_2$ has intriguing magnetic properties.[1−4] It was reported[1] that $PrMnSi_2$ shows a ferromagnetic (FM) ordering of the Mn sublattice up to $T_C = 434$ K and an additional magnetic ordering of the Pr sublattice at low temperatures, eventually leading to an antiferromagnetic (AFM) structure below $T_N = 35$ K. According to the neutron diffraction study at 4.2 K,[2] the atoms of each Mn layer are ferromagnetically coupled, with moments perpendicular to the layer, so are those of each Pr layer, and all adjacent Mn and Pr layers are antiferromagnetically coupled to each other. The magnetic moment of Mn at room temperature is approximately 2 $\mu_B$ parallel to the $b$-axis while those of Mn and Pr below 35 K are respectively 2.35 and 2.04 $\mu_B$ parallel to the $b$-axis.[2] In general, rare earth intermetallic compounds $RMnX_2$, $RMn_2X_2$, and $RFe_6X_6$ (R = rare earth, X = main group element) consisting of single layers of transition metal atoms exhibit a long-range magnetic order at high temperatures.[4] In particular, the $RMn_2X_2$ phases, which have been extensively studied during the past 2 decades, exhibit multiple phase transitions associated with magnetic interactions between Mn and Mn, R and Mn, and R and R.[3] The Mn layers of the $RMnX_2$ phases are farther separated than are those of the $RMn_2X_2$ phases.[1,2] Nevertheless, the $RMnX_2$ phases show a long-range magnetic order at high temperatures.[1,2,4] Among the $RMnX_2$ phases that have been studied so far, $PrMnSi_2$ is unique because its magnetic coupling between adjacent Mn layers changes from FM to AFM. The latter accompanies the FM ordering of the Pr moments in each Pr layer. Furthermore, the AFM state of $PrMnSi_2$ can be converted to a FM state upon applying a magnetic field higher than 5 T.[1] To gain insight into these intriguing physical properties of $PrMnSi_2$, we have measured the magnetic susceptibilities of $PrMnSi_2$ for the cooling and warming cycles, the magnetizations of $PrMnSi_2$ with field strength up to 7 T,

† Permanent address: ICMCB−CNRS, 87, avenue du Dr. A. Schweitzer, 33608 Pessac Cedex, France.

(1) Venturini, G.; Malaman, B.; Meot-Meyer, M.; Fruchart, D.; Le Caer, G.; Malterre, D.; Roques, B. *Rev. Chim. Miner.* **1986**, *23*, 162.
(2) Malaman, B.; Venturini, G.; Pontonnier, L.; Fruchart, D. *J. Magn. Magn. Mater.* **1990**, *86*, 349.
(3) Schobinger-Papamantellos, P.; Brabers, J. H. V. J.; de Boer, F. R.; Buschow, K. H. J. *J. Alloys Compd.* **1994**, *203*, 23.
(4) Szytula, A.; Leciejewicz, J. *Handbook of crystal structures and magnetic properties of rare earth intermetallics*; CRC Press: Ann Arbor, 1994.

10.1021/cm050622p CCC: $30.25 
Published on Web 06/16/2005

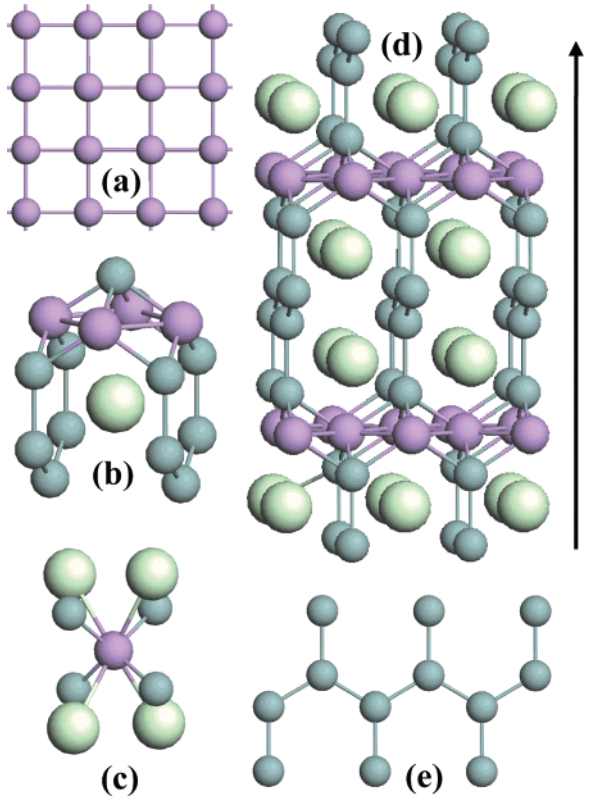


**Figure 1.** Crystal structure of $PrMnSi_2$: (a) a square net of Mn atoms, (b) a Pr atom in a $Si_{10}Mn_4$ cage and a $Mn_4Si$ square pyramid, (c) the coordinate environment of a Mn atom, (d) a perspective view of $PrMnSi_2$ showing the magnetic-atom layer sequence $(-Pr-Mn-Pr-)_\infty$ along the b-direction (indicated by an arrow), and (e) a silicon-ribbon chain.

and the heat capacities of $PrMnSi_2$. Results of our experiments were interpreted by calculating the electronic band structures for several ordered spin states of $PrMnSi_2$.

## 2. Experimental Section

Samples of $PrMnSi_2$ were prepared with the elements purchased from Alfa Aesar: Mn (dendritic pieces, 99.98%), Pr (1-mm thick foil, 99.9%), and Si (lumps, 99.9999%). The Mn pieces were cleaned by etching the surfaces in a $HNO_3$ solution (10 wt %). The oxide on the surface of the Pr foil was scraped off carefully. Stoichiometric amounts of the elements were mixed and fused by arc-melting under an argon environment with a zirconium oxygen-getter. Due to the evaporation of Mn during the arc-melting, the best results were obtained when Mn was loaded in excess (10 at. %). The resulting button was inserted into an $N_2$-filled Ta-tube container, which was later sealed by arc-welding and placed in an evacuated and flame-sealed fused silica tube. The sealed silica tube was heated at 1373 K for 15 days and then cooled radiatively to room temperature. After the reaction, the Ta-tube container showed no visible sign of reaction with the samples.

With the powder X-ray diffraction (XRD) data obtained for the sample used for our property measurements, a Rietveld refinement was carried out. The results of our refinement are summarized in Figure S1 and Table S1 of the Supporting Information. The refined unit cell parameters and atomic positions are in good agreement with those reported by Malaman et al.[2] With inductively coupled plasma atomic emission spectroscopy we also performed an elemental analysis of the sample used for our property measurements. This analysis shows that the bulk composition of the sample is stoichiometric within the experimental error limit, namely, Pr: 56.1(4), Mn: 21.6(4), and Si: 21.9(4) wt %. The corresponding theoretical values are 55.9, 21.8, and 22.3, respectively. The XRD pattern showed a very small Bragg reflection peak at $2\theta = 16.2°$ (Figure S1), which is assigned to $PrMn_2Si_2$. $PrMn_2Si_2$ exhibits an AFM state ($T_N = 368$ K) and does not undergo any phase transition in the temperature region of our measurements.[5,6] Consequently, any significant changes in the magnetic susceptibility of the sample should be associated with $PrMnSi_2$ because the overall magnetic susceptibility of a sample is the sum of the susceptibilities of its components. The same applies to our heat capacity measurements.

The magnetic susceptibilities and magnetizations were measured with a MPMS SQUID magnetometer (Quantum Design, 6325 Lusk Boulevard, San Diego) on a polycrystalline sample of irregular shape. The heat capacities were measured using a commercial Physical Property Measurements System calorimeter (Quantum Design, 6325 Lusk Boulevard, San Diego) employing the relaxation method. To thermally anchor the crystals to the sample holder platform, a minute amount of Apiezon grease was used. The total heat capacity of platform and grease was determined in a separate run and subtracted.

## 3. Magnetic Susceptibility, Magnetization, and Heat Capacity

The magnetic susceptibility $\chi$ measured at the magnetic field $H = 0.1$ T is presented in Figure 2, which shows a strong hysteresis in the cooling and warming cycles. On the cooling cycle, a sharp decrease in $\chi$ occurs at ~50 K and a slope change in the $\chi$-vs-$T$ curve occurs at ~17 K. On the warming cycle, the susceptibility is low at low temperatures up to ~40 K with a small peak at ~14 K and increases sharply above ~50 K. How the hysteresis of the magnetic susceptibility depends on $H$ is presented in Figure 2. The hysteresis nearly disappears at ~5 T, but is present at field $H <$ ~5 T. The susceptibilities of the cooling and warming cycles at 50 K decrease sharply until $H$ reaches 1 T and then decrease slightly (Figure 3), while those at 2 K vary little as a function of $H$ (see the inset of Figure 3). The susceptibility curves at 2 T show deep valleys at 25 K (Figure 2) because the susceptibilities around 25 K do not increase as fast as those at 2 K when $H$ is increased to 2 T. These susceptibility valleys disappear when $H$ is increased beyond 3 T (Figure 2). The latter indicates that the tendency for antiferromagnetism is suppressed at field equal to or greater than 3 T. This is consistent with the result of the magnetization study by Venturini et al.[1]

In the magnetization study of $PrMnSi_2$ by Schobinger-Papamantellos et al.,[3] only the coercivity data were reported at several temperatures. In the present study the magnetization of $PrMnSi_2$ was examined by sweeping the magnetic field up to 7 T at a number of different temperatures. These results are summarized in Figure 4. At all temperatures studied, the magnetization curves exhibit hysteresis. At 35 K and above, each plot shows one hysteresis loop. At 45 K and above, the magnetic moment above 6 T is not saturated but is linear with the magnetic field. At 5 and 20 K, the magnetization curve looks as if it is made up of two weak

(5) Welter, R.; Venturini, G.; Fruchart, D.; Malaman, B. *J. Alloys Compd.* **1993**, *191*, 263.
(6) Elmali, A.; Dincer, I.; Elerman, Y.; Ehrenberg, H.; Fuess, H. *J. Phys.: Condens. Matter* **2004**, *16*, 8669. Sjöstedt, E.; Nordström, L.; Singh, D. *Solid State Commun.* **2000**, *114*, 15.

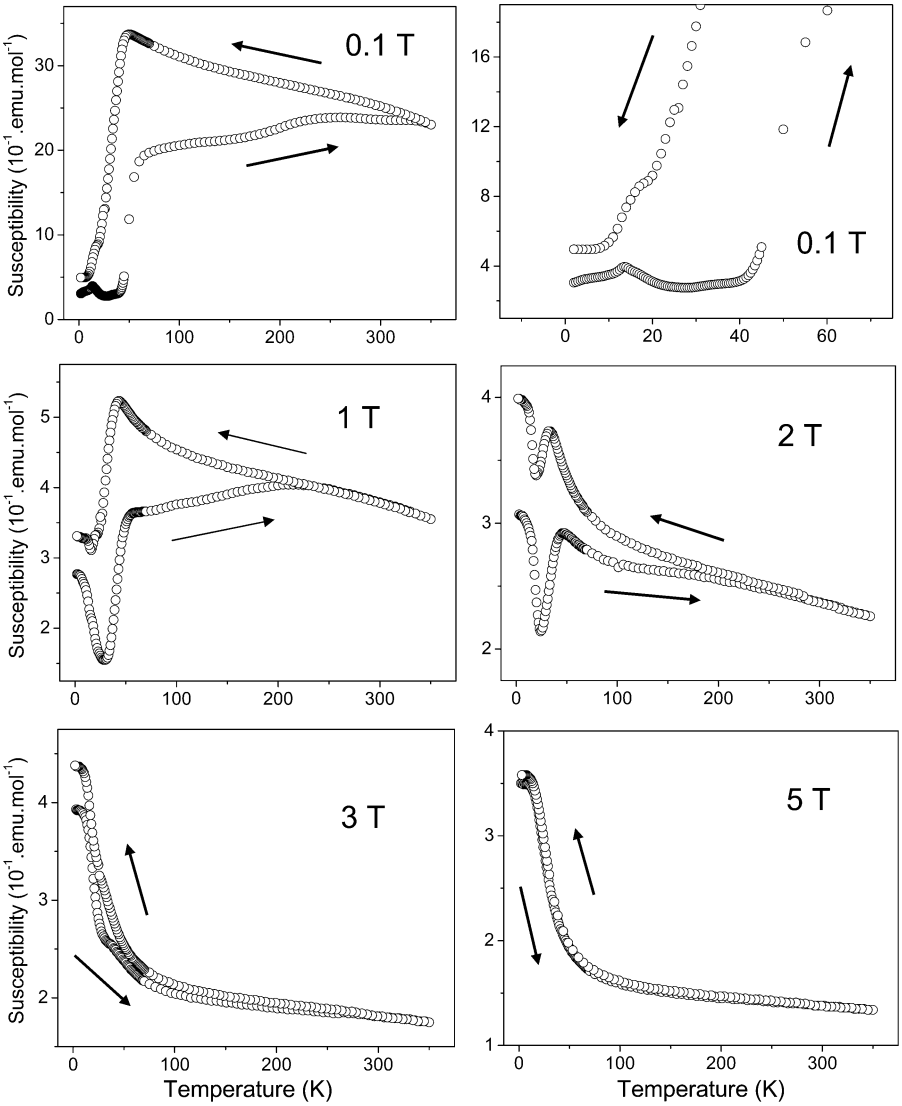


**Figure 2.** Temperature dependence of the magnetic susceptibilities $\chi$ of $PrMnSi_2$ measured for the cooling and warming cycles at various magnetic fields.

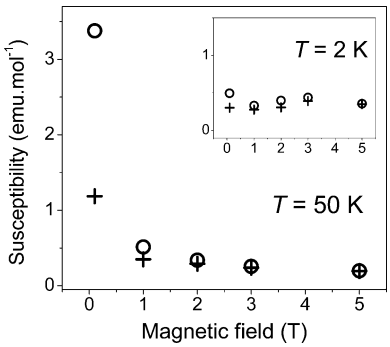


**Figure 3.** Magnetic-field dependence of the magnetic susceptibilities of $PrMnSi_2$ at 50 K. The empty circles refer to the cooling cycle and the crosses to the warming cycle. The corresponding data at 2 K are shown in the inset.

hysteresis loops centered around 3.5 and −3.5 T. Figure 5 shows the magnetization at 7 T, hereafter referred to as the maximum magnetization $M_{max}$, as a function of temperature. $M_{max}$ decreases with increasing temperature, and the $M_{max}$ vs $T$ curve is well fitted by a Gaussian function.

The specific heat $C_p$ of $PrMnSi_2$ measured for the warming cycle is presented in Figure 6 and the corresponding $C_p/T$ plot in the inset of Figure 6. It is noted that the specific heat does not show a prominent feature around 50 K where the magnetic susceptibility curves at low magnetic fields undergo an abrupt change. In contrast, the specific heat shows a prominent feature consisting of two overlapping peaks centered around ∼14 and ∼17 K, where the magnetic susceptibility curves at low magnetic fields exhibit a weak anomaly.

## 4. Electronic Band Structures

Density functional theory (DFT) spin-polarized electronic band structure calculations were carried out for $PrMnSi_2$ using the full-potential augmented plane wave + local orbitals (APW+lo) method[7,8] implemented in the WIEN2k package.[8] The Pr 5s/5p, Mn 3s/3p, and Si 2p orbitals were treated as semi-core states, and the Pr 4d orbitals were treated as core states. To account for the localized character of Pr 4f orbitals, the LDA+$U$ scheme of Anisimov et al.[9] was used

(7) Madsen, G. K. H.; Blaha, P.; Schwarz, K.; Sjöstedt, E.; Nordström, L. *Phys. Rev. B* **2001**, *64*, 195134.
(8) Blaha, P.; Schwarz, K.; Madsen, G. K. H.; Kvasnicka, D.; Luitz, J. *WIEN2k, An Augmented Plane Wave Plus Local Orbitals Program for Calculating Crystal Properties*; Vienna University of Technology: Vienna, Austria, 2001; ISBN 3-9501031-1-2.

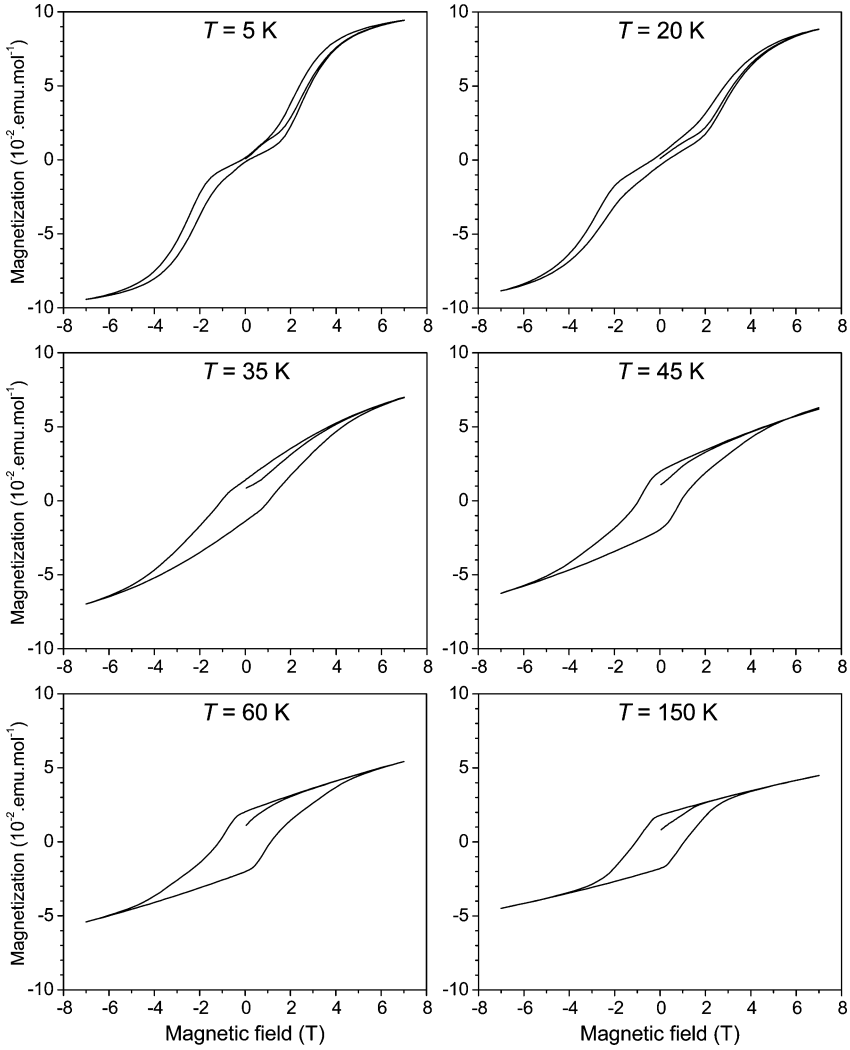


**Figure 4.** Magnetization loops of $PrMnSi_2$ determined at several different temperatures.

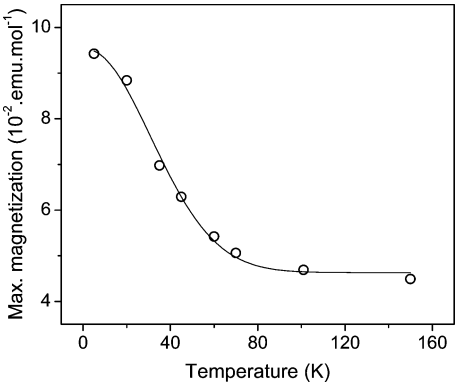


**Figure 5.** Magnetization of $PrMnSi_2$ at 7 T, $M_{max}$, as a function of temperature.

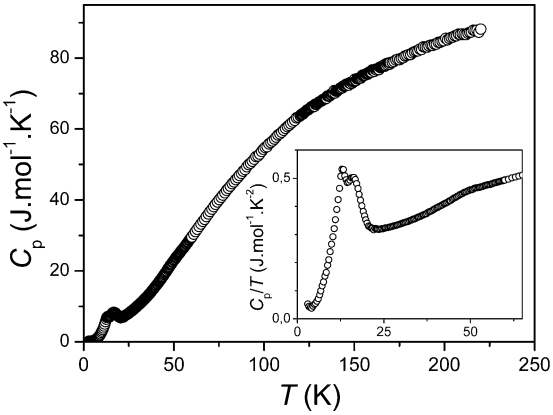


**Figure 6.** Heat capacity $C_p$ of $PrMnSi_2$ as a function of temperature determined for the warming cycle. The inset shows the $C_p/T$ vs $T$ data.

with parameters $U(4f) = 0.5$ Ryd and $J(4f) = 0.05$ Ryd. The plane-wave cutoff was $R_{MT} \cdot K_{max} = 7$, while 60 to 72 $k$-points were used to sample the irreducible Brillouin zones. The atomic sphere radii were set to 2.70 au for Pd, 2.35 au for Mn, and 2.20 au for Si. For our calculations, the crystal structure of $PrMnSi_2$ determined by neutron diffraction at 2 K[2] was employed.

Several ordered spin arrangements of $PrMnSi_2$ were constructed under the assumption that the Mn atoms are ferromagnetically ordered in each Mn layer, and so are the Pr atoms in each Pr layer. These are the FM state and the three different AFM states (i.e., AF1, AF2, and AF3) shown in Figure 7. The AF1 arrangement, in which all adjacent layers of the magnetic atoms are antiferromagnetically coupled, corresponds to the magnetic structure found by the neutron diffraction study at 4.2 K, and hence should be the

(9) Anisimov, V. I.; Solovyev, I. V.; Korotin, M. A.; Czyzyc, M. T.; Sawatsky, G. A. *Phys. Rev. B* **1993**, *48*, 16929.

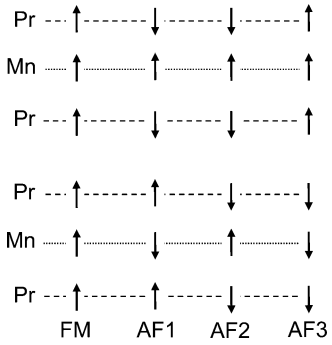


**Figure 7.** Ordered spin arrangements of the ferromagnetically ordered layers of Mn and Pr atoms in the FM, AF1, AF2, and AF3 states.

**Table 1. Relative Energies $\Delta E$ (meV per FU) of Several Ordered Magnetic States of $PrMnSi_2$ and Magnetic Moments on the Mn and Pr Atoms ($\mu_{Pr}$ and $\mu_{Mn}$ in $\mu_B$, Respectively) Calculated by the APW+lo/LDA+$U$ Method Using the Crystal Structures Determined at 2 K**

| | $\mu_{Pr}$ | $\mu_{Mn}$ | $\Delta E$ | | $\mu_{Pr}$ | $\mu_{Mn}$ | $\Delta E$ |
|---|---|---|---|---|---|---|---|
| FM | 2.01 | 1.89 | +178 | AF2 | 2.00 | 1.95 | −1.4 |
| AF1 | 2.01 | 1.94 | 0.0 | AF3 | 2.02 | 1.91 | +11 |

ground state spin arrangement. In the AF2 arrangement, the Mn layers are ferromagnetically coupled, and so are the Pr layers, but the Mn and Pr sublattices are antiferromagnetically coupled. In the AF3 arrangement, adjacent Mn layers are antiferromagnetically coupled, and each Mn layer is ferromagnetically coupled with its two adjacent Pr layers. The relative stabilities of the F, AF1, AF2, and AF3 states calculated for the 2 K structure are summarized in Table 1, and so are the calculated magnetic moments on the Mn and Pr atoms. The plots of the total and partial density of states (DOS) calculated for the AF1 state are shown in Figure 8. The corresponding plots calculated for other ordered spin states exhibit electronic features quite similar to those found for the AF1 state (see below), and hence are not shown.

## 5. Discussion

The linear part of the magnetization curves (Figure 4) at 45 K and above can be understood in terms of the paramagnetism of the Pr atoms. The $M_{max}$ value decreases with increasing temperature (Figure 5) due to the paramagnetism of the Pr atoms because, at a higher temperature, the ordering of the Pr moments along the field direction becomes more difficult. Results of our magnetic susceptibility and heat capacity measurements show that there occur three magnetic phase transitions, one around ∼50 K and two below ∼20 K (i.e., ∼14 and ∼17 K). At 5 K it is most likely that $PrMnSi_2$ adopts the three-dimensional AFM structure found by neutron diffraction at 4.2 K (i.e., the AF1 state in Figure 7). Namely, in the absence of an external magnetic field, the ground magnetic structure at 5 K is AFM so that the overall magnetization should be zero. Thus, the occurrence of two weak hysteresis loops observed at 5 K (Figure 4) reflects a field-induced ferromagnetism. The latter may arise from a spin ordering of the ferromagnetically ordered Mn and Pr layers. If so, it implies that the interlayer AFM interactions are weak and hence this spin arrangement can be easily reversed by an applied field. This view is consistent with the observation that the magnetization shows a saturation behavior at 5 K.

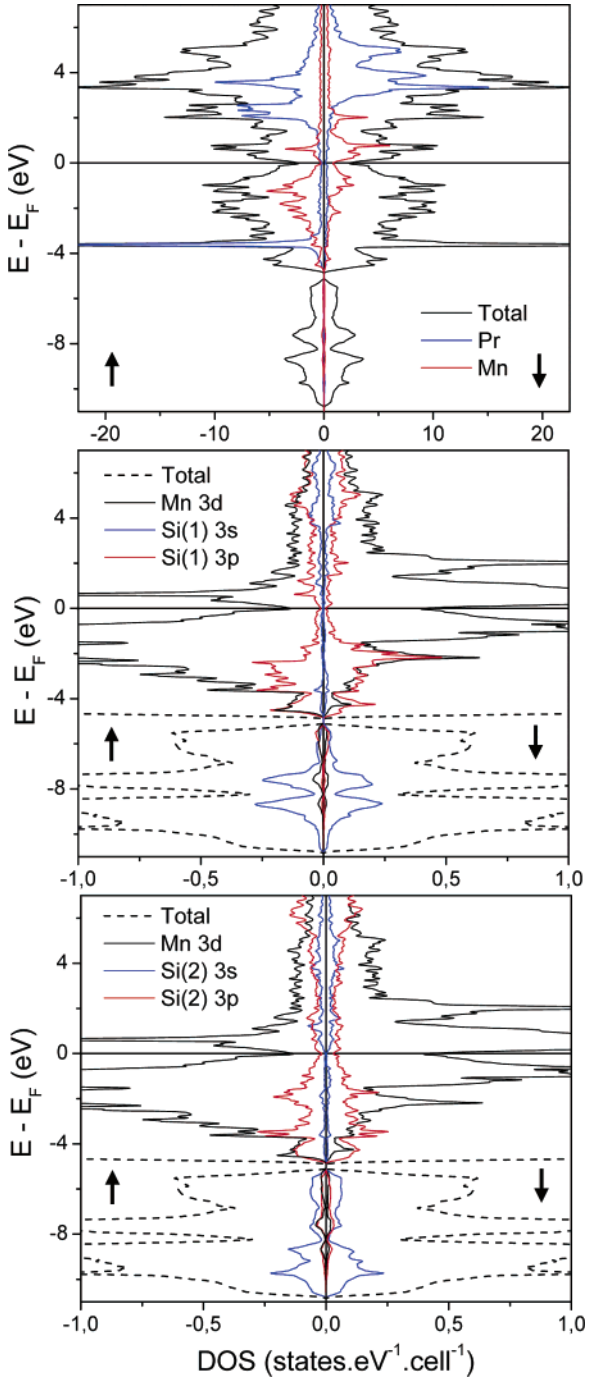


**Figure 8.** Total and projected DOS plots of the AF1 state calculated for the 2 K crystal structure of $PrMnSi_2$ using the APW+lo/LDA+$U$ method. Only the projected DOS plots for the up-spin sites are presented, and those for the down-spin sites are the same as shown except for the switch between the up-spin and down-spin densities. The Si(1) and Si(2) atoms refer to the terminal and inner silicon atoms of the silicon-ribbon chains, respectively.

Although the AF2 state is calculated to be slightly more stable than the AF1 state, the two states are practically the same in stability and constitute the most stable states. The AF3 state is less stable than the AF1 and AF2 states by about 11 meV per formula unit (FU) and the FM state by about 180 meV per FU. The neutron diffraction and the magnetization studies[1,2] of $PrMnSi_2$ reported that the Pr moments in each Pr layer are disordered above 35 K, but are ferromagnetically ordered below 35 K. In other words, an overall AFM ordering occurs when the FM ordering takes place within each Pr layer.

Our electronic structure calculations suggest that the AFM state below ~50 K can be of either the AF1 or the AF2 type. This leads us to speculate on the nature of the magnetic orderings that take place below ~20 K. The AF1 ordering is consistent with the magnetic structure determined at 4.2 K. Thus, the magnetic structure in the temperature region between ~20 and ~50 K might be described by the AF2 ordering. Then, the magnetic transitions that occur below ~20 K could be associated with the transition from the AF2 to the AF1 arrangement. The spin ordering of the Mn sublattice is the same in the FM and AF2 states so that the long-range order of the Mn sublattice is unaffected when the spin ordering of the Pr layers changes from paramagnetic to FM below ~50 K. For the transition from AF2 to AF1, the spins of every second $(-\mathrm{Pr}-\mathrm{Mn}-\mathrm{Pr}-)_\infty$ triple layer should be reversed. This change in the magnetic structure may explain why the $C_p/T$ data show the prominent overlapping peaks below ~20 K. The presence of two overlapping peaks at ~14 and ~17 K can be accounted for if the transition from AF2 to AF1 takes place through another ordered spin state (e.g., a hybrid between AF1 and AF2).

According to our electronic structure calculations, the magnetic moments on the Mn and Pr atoms are approximately 2 $\mu_B$, and the Pr atom carries a slightly larger moment than does the Mn atom (Table 1). These are in good agreement with the experimental observations.[2] According to the DOS plots of Figure 8, the Fermi level lies at the bottom of a DOS valley, hence leading to a very low DOS at the Fermi level (i.e., $N(E_f) \approx 0.6$ states/spin per FU), and the DOS around the Fermi level is dominated by the Mn 3d orbitals with small contributions from the Pr and Si orbitals. These two features are common in the electronic structures of all the ordered spin states considered in our study. Thus, $PrMnSi_2$ is a magnetic metal with low carrier density at the Fermi level so that its electrical resistivity should depend sensitively upon the magnetic order/disorder in the Mn and Pr layers, and hence should exhibit a substantial magnetoresistance.

## 6. Concluding Remarks

The temperature dependence of the magnetic susceptibilities of $PrMnSi_2$ shows a striking hysteresis at low magnetic fields, and the hysteresis persists for magnetic fields up to ~5 T. The magnetic susceptibilities measured at a low magnetic field and the heat capacities show that, in addition to the magnetic phase transition at ~50 K which corresponds to the one reported by Venturini et al.,[1] $PrMnSi_2$ undergoes two additional magnetic phase transitions below ~20 K. The magnetization curves of $PrMnSi_2$ exhibit hysteresis at all temperatures measured. At $T \geq 45$ K the magnetization shows a linear behavior for $H > 6$ T, which is due to the paramagnetism of the Pr atoms. The magnetization at 5 K consists of two weak hysteresis loops centered around 3.5 and −3.5 T, which reflects the occurrence of a field-induced ferromagnetism. The decrease of the maximum magnetization $M_{max}$ with increasing temperature follows a Gaussian function. Our electronic structure calculations show that $PrMnSi_2$ is a magnetic metal with low carrier density at the Fermi level and with magnetic moments of approximately 2 $\mu_B$ on the Mn and Pr atoms. Therefore, the electrical resistivity of $PrMnSi_2$ is expected to show a sensitive dependence on the magnetic order/disorder in the Mn and Pr layers and hence exhibit a substantial magnetoresistance. Our calculations suggest that the magnetic transition below ~20 K could be associated with the transition from the AF2 to the AF1 arrangement. Further experimental and theoretical studies are necessary to fully characterize the nature of the magnetic phase transitions of $PrMnSi_2$ below ~50 K.

**Acknowledgment.** The work at North Carolina State University was supported by the Office of Basic Energy Sciences, Division of Materials Sciences, U.S. Department of Energy, under Grant DE-FG02-86ER45259, and the work at Arizona State University by National Science Foundation through the CAREER Award to D.-K. S. (DMR, Contract No. 0239837). The authors are grateful to E. Brücher for measurement of the magnetic data. Computational facilities were provided by the Pole M3PEC, Bordeaux 1 University.

**Supporting Information Available:** Figure S1 of the observed and calculated XRD profiles and Table S1 of the refined structural parameters (PDF). This material is available free of charge via the Internet at http://pubs.acs.org.

CM050622P